

Monte Carlo simulation for fragment mass and kinetic energy distributions from the neutron-induced fission of ^{235}U

M. Montoya^{a,b}, E. Saettone^b, and J. Rojas^{a,c}

^a Instituto Peruano de Energía Nuclear, Av. Canadá 1470, Lima 41, Perú.

^b Facultad de Ciencias, Universidad Nacional de Ingeniería, Av. Tupac Amaru 210, Apartado 31-139, Lima, Perú.

^c Facultad de Ciencias Físicas, Universidad Nacional Mayor de San Marcos, Av. Venezuela s/n, Apartado Postal 14-0149, Lima - 14, Perú.

Recibido el 8 de enero de 2007; aceptado el 23 de agosto de 2007

The mass and kinetic energy distribution of nuclear fragments from the thermal neutron-induced fission of ^{235}U have been studied using a Monte Carlo simulation. Besides reproducing the pronounced broadening on the standard deviation of the final fragment kinetic energy distribution ($\sigma_e(m)$) around the mass number $m = 109$, our simulation also produces a second broadening around $m = 125$ that is in agreement with the experimental data obtained by Belhafaf *et al.* These results are a consequence of the characteristics of the neutron emission, the variation in the primary fragment mean kinetic energy, and the yield as a function of the mass.

Keywords: Monte Carlo; neutron induced fission; ^{235}U ; standard deviation.

Mediante la simulación con el método Monte Carlo, fue estudiada la distribución de masas y energía cinética de los fragmentos de la fisión inducida por neutrones térmicos del ^{235}U . Además de reproducir el ensanchamiento pronunciado en la desviación estándar de la distribución de la energía cinética de los fragmentos finales ($\sigma_e(m)$) alrededor del número másico $m = 109$, nuestra simulación también produce un segundo ensanchamiento alrededor de $m = 125$, en concordancia con los datos experimentales obtenidos por Belhafaf *et al.* Estos resultados son consecuencia de las características de la emisión de neutrones, la variación de la energía cinética media y el rendimiento de los fragmentos primarios en función de la masa.

Descriptores: Monte Carlo; fisión inducida por neutrones; ^{235}U ; desviación estándar.

PACS: 21.10.Gv; 25.85.Ec; 24.10.Lx

1. Introduction

Since the discovery of the neutron-induced fission of uranium by Hahn and Strassmann in 1938 [1], a great effort has been made to understand the processes involved in it and to measure the relevant fission parameters. Nowadays several aspects of heavy nuclei fission seem to be clarified. Meitner and Frisch suggested a theoretical explanation based on a nuclear liquid-drop model [2], and, over the past 30 years the model has provided considerable insight into nuclear structure [3]. It is known that the de-excitation by fission of heavy nuclei depends on the quantum properties of the saddle point and of the associated fission barrier. The detection of fission isomers has been interpreted by the secondary well in the fission barrier [4]. The nascent fragments begin to be formed at the saddle point, then the system falls to the fission valley (energetically preferred paths to fission) and ends at the scission configuration, where fragments interact only by Coulomb force. Moreover, at scission, the fragments have acquired a pre-scission kinetic energy. Over the fission valley, the system could be described by collective variables (such as deformation, vibration, rotation, etc.) and intrinsic variables (such as quasi-particle excitations).

Nevertheless, the dynamics of the fission processes are not yet completely understood [5]. In particular, the nature of the coupling between the collective and intrinsic degrees of freedom during the descent from the saddle to scission is

not known either, nor is it known how it arises. The physics problem of the description of the fission fragment mass and kinetic energy distributions is very closely related to the topological features in the multi-dimensional potential energy surface [6]. In low-energy fission, several final fragment characteristics can be explained in terms of a static scission model of two coaxial juxtaposed deformed spheroidal fragments, providing shell effects, affecting the deformation energy of the fragments.

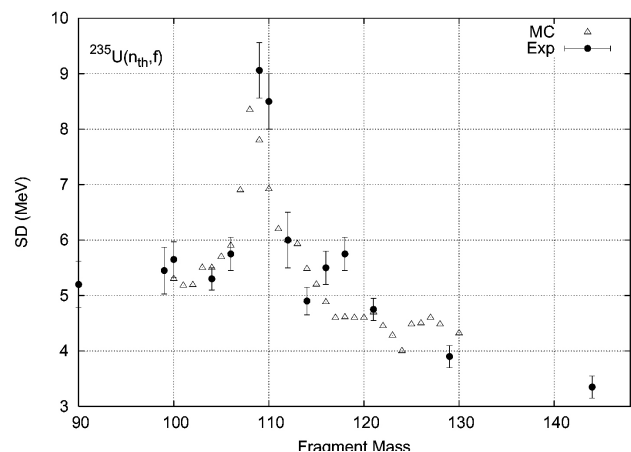


FIGURE 1. Thermal neutron induced fission of ^{235}U . Standard deviation of the final fragment kinetic energy distribution as a function of the final mass m , as a result of Monte-Carlo simulation (Δ), and experimental data (\bullet). Both from [9].

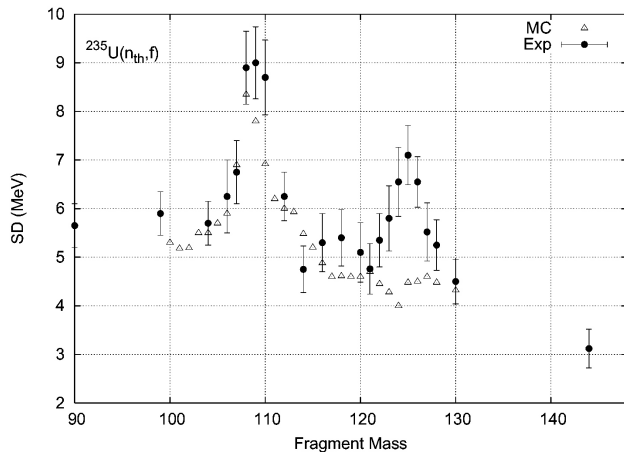


FIGURE 2. Thermal neutron-induced fission of ^{235}U . Simulated standard deviation of the final fragment kinetic energy distribution as a function of the final mass m (Δ), from Ref. 9, does not reproduce the experimental broadening around $m = 125$, taken from Ref. 10.

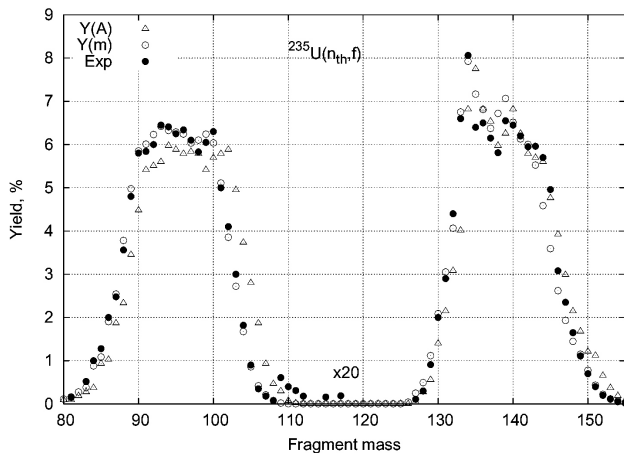


FIGURE 3. Thermal neutron-induced fission of ^{235}U . Simulation results for the primary (Δ) and final (\odot) mass yields are presented together with experimental data (\bullet), taken from Ref. 11.

These shell effect corrections, determined by the Strutinsky prescription and discussed by Dickmann *et al.* [7] and Wilkins [8], subsequently generate secondary minima in the total potential energy surface corresponding to fragments having some particular neutron or proton shell configurations. If the final fragment characteristics were governed by the properties of the fragments themselves, a basic argument in any statistical theory, one would then expect an increase in the width of the kinetic energy distribution curve for fragment masses A having the above-mentioned special neutron or proton shell arrangements. In order to address this question, the fission parameters of the primary fragments (pre-neutron emission) that have been most studied are the mass yield ($Y(A)$) and the kinetic energy ($E(A)$) distribution.

Nevertheless, direct measurements can only be carried out on the final fragments (post neutron emission) mass yield $Y(m)$ and kinetic energy ($e(m)$). Therefore it is crucial to find out what the relation is between the primary and the fi-

nal kinetic energy distributions, as well as the relation between the $Y(A)$ and $Y(m)$ curves. For thermal neutron-induced fission of ^{235}U , which in fact is the fission of excited ^{236}U ($^{236}\text{U}^*$) formed by neutron absorption by ^{235}U , the $e(m)$ distribution was experimentally determined by Brissot *et al.* [9]. This distribution was represented by the mean value of kinetic energy \bar{e} and the standard deviation (SD) of the kinetic energy σ_e as a function of the final mass m . As seen in Fig. 1, the plot of both the measured values and the results of a Monte Carlo simulation of σ_e from a primary distribution $E(A)$ without broadenings, shows a pronounced broadening around $m \approx 109$. This Monte Carlo simulation result suggests that the broadening does not exist on the primary fragment kinetic energy as a function of the primary fragment mass.

In a later experiment, Belhafaf *et al.* [10], repeated the experiment of Brissot *et al.* for neutron-induced fission of ^{235}U , obtaining a second broadening around $m \approx 125$ (see Fig. 2). A Monte Carlo simulation made by these authors, from a primary distribution of $E(A)$ without a broadening, reproduced the experimental broadening on σ_e at $m = 109$, but failed to reproduce the broadening around $m = 125$. They suggested that this broadening must exist in the primary fragment kinetic energy ($E(A)$) distribution, and accordingly they fitted their experimental data from a distribution with a broadening around $A=126$.

In this paper, we present new Monte Carlo simulation results for thermal neutron-induced fission of ^{235}U . We compute both the mass and kinetic energy of the primary and final fission fragments, and we show that the broadenings on the σ_e curve around the final fragment masses $m = 109$ and $m = 125$ can be reproduced without assuming an adhoc initial structure on the $\sigma_E(A)$ curve.

2. Monte Carlo simulation model

2.1. Fragment kinetic energy and neutron multiplicity

In the process of thermal neutron-induced fission of ^{235}U , the excited composed nucleus $^{236}\text{U}^*$ is formed first. Then, this nucleus splits into two complementary fragments having A_1 and A_2 as mass numbers, and E_1 and E_2 as kinetic energies, respectively.

Using relations based on momentum and energy conservation, the total kinetic energy of complementary fragments turns out to be

$$TKE = E_1 + E_2 = \frac{A_1 + A_2}{A_2} E_1. \quad (1)$$

The total excitation energy is given by

$$TXE = Q - \epsilon_n - TKE, \quad (2)$$

where Q is the difference between the fissioning nucleus mass and the sum of two complementary fragments masses, and ϵ_n is the separation neutron energy of ^{236}U . Using

Eq. (1) in (2) and taking into account that $A_1 + A_2 = 236$ gives

$$TXE = Q + \epsilon_n - \frac{236}{236 - A}E, \tag{3}$$

where A and E are the mass number and kinetic energy, respectively, of one of the two complementary fragments. It is reasonable to assume that the excitation energy of one complementary fragment (E^*) is proportional to the total excitation energy, so that,

$$E^* \propto TXE = Q + \epsilon_n - \frac{236}{236 - A}E, \tag{4}$$

and that the number (ν) of neutrons emitted by a fragment is proportional to its excitation energy, *i.e.*

$$\nu \propto E^*. \tag{5}$$

From relations (4) and (5), one derives a linear relation between ν and E :

$$\nu = a + bE. \tag{6}$$

Taking into account that there is no neutron emission $\nu = 0$ for fragments having the maximal kinetic energy (E_{max}), and assuming that for the average value of fragment kinetic energy $\nu = \bar{\nu}$, relation (6) turns out to be

$$\nu = \bar{\nu} \left(\frac{E_{max} - E}{E_{max} - \bar{E}} \right). \tag{7}$$

Let β be the parameter that defines the maximal value of kinetic energy by the relation

$$E_{max} = \bar{E} + \frac{\sigma_E}{\beta}. \tag{8}$$

Then, relation (7) may be expressed as

$$\nu = \bar{\nu} \left(1 - \beta \left(\frac{E - \bar{E}}{\sigma_E} \right) \right). \tag{9}$$

Because the neutron number N is an integer, it will be defined as the integer part of (9), *i.e.*

$$N = \text{Integer part of} \left(\alpha + \bar{\nu} \left(1 - \beta \left(\frac{E - \bar{E}}{\sigma_E} \right) \right) \right), \tag{10}$$

where α is used to compensate for the effect of the change from a real number ν to an integer number N .

2.2. Simulation process

In our Monte Carlo simulation, the input quantities are the primary fragment yield (Y), the average kinetic energy (\bar{E}), the standard deviation of the kinetic energy distribution (σ_E), and the average number of emitted neutron ($\bar{\nu}$) as a function of primary fragment mass (A). The output of the simulation for the final fragment are the yield (Y), the standard deviation of the kinetic energy distribution (σ_E) and the average number of emitted neutrons ($\bar{\nu}$) as a function of final fragment mass m .

For the first simulation, we take Y from Ref. 11, $\bar{\nu}$ from experimental results by Nishio *et al.* 12, and \bar{E} from Ref. 10. The first standard deviation σ_E curve is taken without any broadening as a function of A . Then, we adjust $Y(A)$, $\nu(A)$, $\bar{E}(A)$ and $\sigma_E(A)$ in order to get $Y(m)$, $\bar{\nu}$, $\bar{e}(m)$, $\sigma_e(m)$ in agreement with experimental data.

In the simulation, for each primary mass A , the kinetic energy of the fission fragments is chosen randomly from a Gaussian distribution

$$P(E) = \frac{1}{\sqrt{2\pi}\sigma_E} \exp \left[-\frac{(E - \bar{E})^2}{2\sigma_E^2} \right], \tag{11}$$

where $P(E)$ is the probability density of energy with mean value \bar{E} and standard deviation σ_E .

For each E value, the simulated number of neutrons N is calculated with relation (10). The final mass of the fragment will be

$$m = A - N. \tag{12}$$

Furthermore, assuming that the fragments lose energy only by neutron evaporation and not by gamma emission or any other process, and neglecting the recoil effect due to neutron emission, then the kinetic energy $e(m)$ of the final fragment will be given by

$$e(m) = \left(1 - \frac{N}{A} \right) E. \tag{13}$$

With the set of values corresponding to m , e and N , we calculate $Y(m)$, $\bar{e}(m)$, $\sigma_e(m)$ and $\nu(m)$.

On the other hand, to obtain acceptable statistics during the simulation, we have considered a total number of fission events of ^{235}U of the order of 10^8 . At the same time, we have used the Box-Muller method to generate the random numbers with the required normal distribution [13], and have computed the SD of all the relevant quantities by means of the following expression which for $e(m)$, reads as

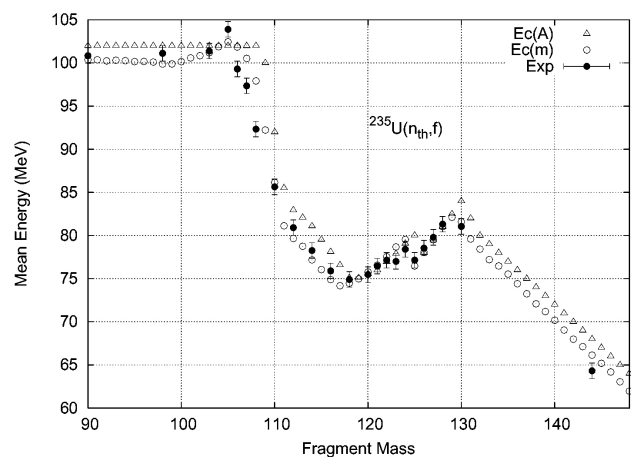


FIGURE 4. Thermal neutron-induced fission of ^{235}U . Mean kinetic energy of the final fragment (\odot) and the mean kinetic energy of the primary fragments \triangle , as a result of simulation in this work, to be compared experimental data (\bullet) taken from Ref. 10.

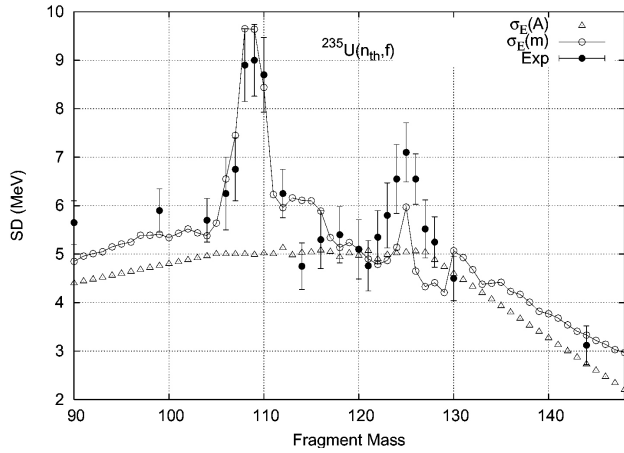


FIGURE 5. Thermal neutron induced fission of ^{235}U . Standard deviation of final fragment kinetic energy distribution (\odot) and standard deviation of primary fragment kinetic energy distribution (\triangle), as simulated in this work, to be compared with experimental data (\bullet) from Ref. 10.

$$\sigma^2(m) = \frac{\sum_{j=1}^{N_j(m)} e_j^2(m)}{N_j(m)} - \bar{e}^2(m), \quad (14)$$

where $\bar{e}(m)$ is the mean value of the kinetic energy of final fragments with a given mass m , and $N_j(m)$ is the number of fission events corresponding to that mass.

3. Results and discussion

The simulated final mass yield curve $Y(m)$ and the primary mass yield curve $Y(A)$ are illustrated in Fig. 3. As expected, due to neutron emission, the $Y(m)$ curve is shifted from $Y(A)$ towards smaller fragment masses. As stated in Sec. 2, the primary kinetic energy ($E(A)$) is generated from a Gaussian distribution, while the final kinetic energy ($e(m)$) is calculated by Eq. (13). The plots of the simulated mean kinetic energy for the primary and final fragments as a function of their corresponding masses, are shown in Fig. 4. In general, the simulated average final kinetic energy curve as a function of final mass ($\bar{e}(m)$) undergoes a shift roughly similar to that of the $Y(m)$ curve, with a diminishing given by relation (13) with $N = \bar{\nu}$. The exceptions to this rule are produced in mass regions corresponding to variations in the slope of $Y(A)$ or $\bar{E}(A)$ curves, for example for $A = 109$, $A = 125$ and $A = 130$. Furthermore, Fig. 5 displays the standard deviation of the kinetic energy distribution of the primary fragments and the standard deviation of the kinetic energy of the final fragments ($\sigma_e(m)$). The plots of $\sigma_e(m)$ reveal the presence of a pronounced broadening around $m = 109$, and a second broadening is found around $m = 125$ in a mass region where there are variations in the slopes of the $Y(A)$ or $\bar{E}(A)$ curves. There are no experimental data around $m = 130$. Nevertheless, if one takes the experimental value $\sigma_e = 3.9\text{MeV}$ for $m = 129$ from Ref. 9 and puts it into Fig. 5, the beginning of another broadening for $m = 130$ is suggested.

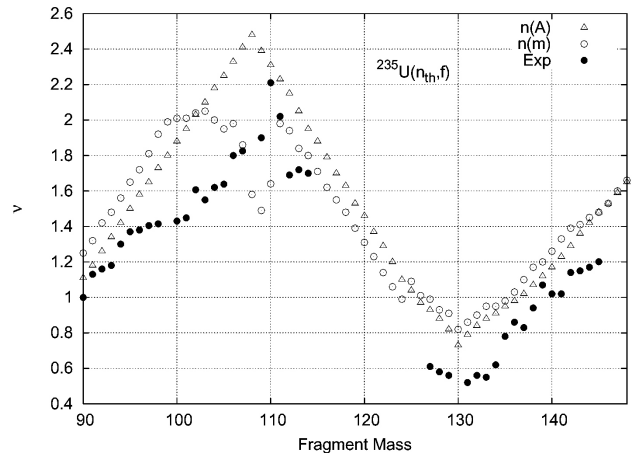


FIGURE 6. The average number of emitted neutrons from the fission of ^{235}U : as a function of the primary fragment mass A (\triangle), as a function of final fragment mass (\odot) both as a result of simulation and experimental data (\bullet), taken from Ref. 12.

These results were obtained with a simulated primary fragment kinetic energy distribution (see Fig. 6, \triangle) without broadenings in the range of fragment masses A from 90 to 145. If one simulates an additional source of energy dispersion in σ_E , without any broadening, no broadening will be observed in σ_e .

Both the shape and height of the broadenings of $\sigma_e(m)$ are sensitive to the value of parameters α and β appearing in Eq. (10). A higher value of α will produce a larger broadening of SD. The effect of β on the broadening depends to a great extent on the mass region. For the region $m = 109$, a higher value of β will produce a greater broadening of SD. The simulated results for $\sigma_e(m)$ presented in Fig. 5 were obtained with $\alpha = 0.62$ and $\beta = 0.35$.

The simulated average number of emitted neutron $\bar{\nu}(m)$ curve is shifted from $\bar{\nu}(A)$ in a similar way as $Y(m)$ relative to $Y(A)$ (see Fig. 6). The presence of broadenings about $m = 109$ could be associated with neutron emission characteristics (approximately $\bar{\nu} = 2$) and a very sharp fall in kinetic energy from $E = 100\text{ MeV}$ to $E = 85.5\text{ MeV}$, corresponding to $A = 109$ and $A = 111$, respectively. The second broadening is produced by a discontinuity in the curve $\bar{E}(A)$ between $A = 126$ and $A = 125$, which is necessary to reproduce a similar discontinuity between $m = 125$ and $m = 124$. We place special emphasis on the shape of σ_e which increases from $m = 121$ to $m = 125$ and decreases from $m = 125$ to $m = 129$, as occurs with experimental data.

4. Conclusion

Using a simple model for the neutron emission by fragments, we have carried out a Monte-Carlo simulation for the mass and kinetic energy distributions of final fragments from the thermal neutron-induced fission of ^{235}U . In comparison with the primary fragments, the final fission fragments have eroded kinetic energy and mass values, to the point of giving rise to the appearance of broadenings in the standard

deviation of the final fragments kinetic energy as a function of mass $\sigma_e(m)$ around $m = 109$ and $m = 125$ respectively. These broadenings are a consequence of neutron emission and variations on slopes of primary fragment yield $Y(A)$ and

mean kinetic energy $\bar{E}(A)$ curves. From our simulation results, another broadening, around $m = 130$, may be predicted.

-
1. O. Hahn and F. Strassmann, *Naturwissenschaften* **27** (1939) 11.
 2. L. Meitner and O. R. Frisch, *Nature (London)* **143** (1939) 239.
 3. K. Pomorski and J. Dudek, *Phys.Rev.C* **67** (2003) 044316.
 4. M. Bostereli, E.O. Fiset, J.R. Nix, and J.L. Norton, *Phys. Rev. C* **5** (1972) 1050.
 5. K.H. Schmidt, J. Benlliure, and A.R. Junghans, *Nucl.Phys. A* **693** (2001) 169.
 6. P. Möller, D.G. Madland, A.J. Sierk, and A. Iwamoto, *Nature* **409** (2001) 785.
 7. F. Dickmann and K. Dietrich, *Nucl. Phys. A* **129** (1969) 241.
 8. B. D. Wilkins, E.P. Steinberg, and R.R. Chasman, *Phys. Rev. C* **14** (1976) 1832.
 9. R. Brissot *et al.*, *Proc- 4th Symp. On Physics and Chemistry of Fission; Juelich, 1979* (IAEA, Vienna, 1980) Vol. 2, p.99.
 10. D. Belhafaf *et al.*, *Z. Physik A - Atoms and Nuclei* **309** (1983) 253.
 11. C. Wagemans, *The Nuclear fission Process CRC Press, Brussels* (1998) 288.
 12. K. Nishio, Y. Nakagome, H. Yamamoto, and I. Kimura *Nucl. Phys. A* **632** (1998) 540.
 13. M.M. Woolfson and G.J.Pert, *An Introduction to Computer Simulation* (Oxford University Press, 1999).